

More on the Effect of Vacancies on Metal Characteristics. Work Function and Surface Energy

V. V. Pogosov*

Zaporozhye National Technical University, Zaporozhye, 69063 Ukraine

*e-mail: vpogosov@zntu.edu.ua

Received September 4, 2018

Abstract—Within the density functional method, a simple method for determining the dependence of the work function of electrons and specific surface energy of the metal on the relative density of internal vacancies c_v is proposed. Preserving the style of the stabilized jellium model, the preliminarily calculated volume shift of the conductivity zone bottom $\varepsilon^{(0)} \propto c_v$ in a specific homogeneous metal is introduced into a one-dimensional functional as the zero-point energy. Using the quantity c_v as a small parameter, linear corrections to the abovementioned quantities are found. The expansion coefficients are expressed in terms of characteristics of a defectless metal. Calculations for Na and Al are carried out by the Kohn–Sham method. Temperature dependences of Al characteristics have been constructed in the thermodynamic limit.

DOI: 10.1134/S1063783419020197

1. INTRODUCTION

Characteristics of a metal are sensitive to the presence of defects [1–3]. The effect of thermal vacancies on the specific resistance ρ of a metal is determined experimentally by the residual resistance. Assuming that contributions to the electron scattering by different low-density defects are additive (the Matthiessen rule) [1] and based on the thermodynamic definition of the concentration of vacancies, the dependence of electrical resistance on the density of vacancies can be represented in the form

$$\rho(c_v) = \rho^0(1 + \alpha_p c_v), \quad (1)$$

where ρ^0 is the resistance at room temperature. Using the known values $\rho^0 = 4.70 \times 10^{-8}$ and $2.82 \times 10^{-8} \Omega \text{ m}$ [2], we have intervals of experimental values of the coefficient $\alpha_p = 40\text{--}44$ and $39\text{--}100$ for Na and Al, respectively. Dependence (1), along with the temperature dependence of the resistance, is most interesting near the melting point, where the concept of a vacancy is still quite definite for the crystalline state and vacancy concentrations are maximum. After melting, one should probably speak of “quasi-vacancies” the concentration of which increases further with an increase in temperature [4].

For electrons, a vacancy in a metal is a potential hill; for positrons, a well. Phases of electron wave scattering by a monovacancy were calculated many times in different approximations. In particular, using the Kohn–Sham method, we also found phases of electron scattering by a single vacancy [5]. This allowed us

to estimate the vacancy contribution to the electrical resistance: $\alpha_p = 39$ and 29 for Na and Al, respectively.

The presence of a system of vacancies noncorrelated and ordered in a superlattice in a homogeneous metal (without regard to the surface) causes shifts of the conductivity zone bottom $\varepsilon^{(0)}$. The calculated scattering phases also allow us to determine the shifts for electrons [5] and positrons [6]. The quantity $\varepsilon^{(0)}$ can be characterized as a reference point for the electron energy in a defect metal. The approach proposed in [7, 8] additionally takes into account the solution of a variational problem for an inhomogeneous metal with a homogeneous bulk the density of which is lower due to the presence of vacancies. Based on intuitive considerations, the effective work function W_{eff} of metal electrons was represented as the sum

$$W_{\text{eff}} = W + \delta W_v^{\text{bulk}}, \quad (2)$$

where W is a characteristic calculated by the density functional method and consisting of the bulk component and surface dipole barrier, and

$$\delta W_v^{\text{bulk}} = -\varepsilon^{(0)}.$$

Dependences of form (1) for the electron work function, metal surface energy, and vacancy formation energy by measurements of the temperature dependence for these quantities yet were not present. The dependence just on the quantity c_v yields information about the interaction of vacancies and is of interest for nonequilibrium situations. In early experiments with metal systems [9], self-arbitrary ordering of vacancies

Table 1. Values calculated by the Kohn–Sham method for a defectless metal (components in formulas (29)–(32)) and vacancy coefficients α_W and α_σ

Metal	r_s^0, a_0	W^0, eV	$\frac{\Delta W}{\Delta \bar{n}} \bar{n}^0, \text{eV}$	$\frac{\varepsilon^{(0)}}{c_v}, \text{eV}$	α_W	$\sigma^0, \text{erg/cm}^2$	$\frac{\Delta \sigma}{\Delta \bar{n}} \bar{n}^0, \text{erg/cm}^2$	α_σ
Na	3.99	2.93	0.63	4.10	−1.61	171	169	−3.77
Al	2.07	4.30	0.56	13.3	−3.22	926	592	−9.77

was observed, which clearly points to the manifestation of correlations between them. For example, for a simple cubic superlattice and concentrations with $c_v \geq 10^{-3}$, each of the vacancies undergoes a significant action from the field of tails of Friedel oscillations of the electron density from nearest neighbor vacancies [5]. In polyhedral clusters with $N \geq 100$ atoms, diffusion of vacancies along ridges is observed during surface melting (premelting) [10, 11]; with an increase in temperature, diffusion of surface vacancies into the bulk is also possible [12]. The presence of even one internal vacancy at $N = 100$ leads to an anomalously large value $c_v = 10^{-2}$, and the cluster itself becomes a vacancy elementary cell.

This work is aimed at adapting the popular stabilized jellium model [13, 14] of a defectless metal to a metal containing vacancies, as well as at justifying and constructing a consistent procedure of finding the vacancy dependence of form (1) for the electron work function and surface energy with the preservation of the style inherent to the stabilized jellium model.

2. DEFECTLESS METAL

In the stabilized jellium (SJ) model, the energy of a large spherical defectless metal cluster containing N atoms and situated in vacuum is written in the form of the inhomogeneous electron density functional $n(r)$:

$$E_N[n(r)] = \frac{e}{2} \int dr \phi(r) [n(r) - n_+(r)] + G_N[n(r)] - \tilde{\varepsilon} \int dr n_+(r) + \langle \delta v \rangle_{\text{WS}} \int dr \theta(r - R_N) n(r), \quad (3)$$

where e is the unit positive charge and $\phi(x)$ is the electrostatic potential in the usual jellium (J) model [15]; the distribution of negative $n(r)$ and positive

$$n_+(r) = \bar{n} \theta(r - R_N) \quad (4)$$

charges is one-dimensional; $\theta(x) = \{1, x \leq 0; 0, x > 0\}$ is the unit step Heaviside function; and

$$\bar{n} = \left(\frac{4}{3} \pi r_s^3 \right)^{-1} \quad (5)$$

is the electron density in the bulk. Here, r_s is the average distance between electrons of a homogeneous (defectless) metal and the cluster radius in the liquid drop model

$$R_N = N^{1/3} r_0, \quad (6)$$

where $r_0 = Z^{1/3} r_s$ is the Wigner–Seitz cell radius and Z is the valence of the metal.

In expression (3), the total energy functional $E_N[n]$ is associated with the energy $\varepsilon = \varepsilon_J + \varepsilon_M + \bar{\omega}_R$ per one electron; the universal functional $G_N[n]$, with the energy of the usual jellium ε_J equal to the sum of the kinetic (ε_t) and exchange–correlation (ε_{xc}) energies [16]; $\tilde{\varepsilon} = 3Ze^2/5r_0$ is the self-repulsion energy of the positively charged background in each Wigner–Seitz cell

$$\langle \delta v \rangle_{\text{WS}} = \tilde{\varepsilon} + \varepsilon_M + \bar{\omega}_R \quad (7)$$

is the cell volume averaged difference between the ion lattice pseudopotential and electrostatic potential of the positively charged background;

$$\varepsilon_M = -9Ze^2/10r_0 \quad (8)$$

is the average Madelung energy or the electrostatic energy of a system of point ions immersed into a homogeneous negatively charged background with a density \bar{n} ;

$$\bar{\omega}_R = 2\pi e^2 \bar{n} r_c^2 \quad (9)$$

is the average magnitude of the non-Coulomb part of the Ashcroft pseudopotential, r_c is the core radius [13]. The quantity r_c is evaluated from the condition

$$P = 0 \quad (10)$$

for the pressure P in metals as $R_N \rightarrow \infty$ and equilibrium (experimental) values r_s^0 (see Table 1 in [25]).

Here and below, the overbar denotes values of the quantities in a bulk of a homogeneous metal. All characteristics of a defectless cluster are determined as a result of minimizing one-dimensional functional (3).

The input data of the model are r_s and Z . We recall that the quantity $\langle \delta v \rangle_{\text{WS}}$ is strongly different for different metals. For example, $\langle \delta v \rangle_{\text{WS}} = -0.06$ and -2.49 eV for Na and Al, respectively.

3. INTERNAL VACANCIES IN A METAL

Following the mechanism of vacancy blowing, we assume that the number of atoms in the sample does not depend on the presence of vacancies; the density of atoms in the intervacancy bulk is the same as in the absence of vacancies [7, 8] and the vacancies are distributed in the form of a superlattice.

The energy of a sphere containing N atoms and N_v vacancies the centers of which are determined by radius vectors \mathbf{R}_i is written in the form of the functional

$$E_{N,v}[n(\mathbf{r})] = \frac{e}{2} \int d\mathbf{r} \phi(\mathbf{r}, \mathbf{R}_i) [n(\mathbf{r}, \mathbf{R}_i) - n_+(\mathbf{r}, \mathbf{R}_i)] + G[n(\mathbf{r}, \mathbf{R}_i)] - \tilde{\epsilon} \int d\mathbf{r} n_+(\mathbf{r}, \mathbf{R}_i) + \langle \delta v \rangle_{\text{WS}} \int d\mathbf{r} [\theta(r - R_{N,v}) - \theta(|\mathbf{r} - \mathbf{R}_i| - r_0)] n(\mathbf{r}, \mathbf{R}_i), \quad (11)$$

$$i = 1, 2, \dots, N_v.$$

The sphere radius $R_{N,v} > R_i$ is determined from the condition

$$\frac{4}{3} \pi R_{N,v}^3 = (N + N_v) \frac{4}{3} \pi r_0^3; \quad (12)$$

$$R_{N,v} = R_N (1 + c_v)^{1/3}, \quad c_v = N_v/N \ll 1.$$

Preserving the style of the SJ model, one can write the spatial distribution of charges in expression (11) for a defect cluster in the form

$$n_+(\mathbf{r}, \mathbf{R}_i) = \bar{n} \theta(r - R_{N,v}) + \delta n_+(\mathbf{r} - \mathbf{R}_i),$$

$$\delta n_+(\mathbf{r}, \mathbf{R}_i) = -\bar{n} \theta(|\mathbf{r} - \mathbf{R}_i| - r_0), \quad (13)$$

$$n(\mathbf{r}, \mathbf{R}_i) = n(r - R_{N,v}) + \delta n(\mathbf{r} - \mathbf{R}_i).$$

The electron distribution is not three-dimensional, but one-dimensional only for the vacancy situated in the center of the sphere: $\delta n = \delta n(|\mathbf{r} - \mathbf{R}_i|)$. The charge distribution satisfies the normalization conditions

$$\int d\mathbf{r} n(r - R_{N,v}) = Z(N + N_v),$$

$$\int d\mathbf{r} \delta n(\mathbf{r} - \mathbf{R}_i) = \int d\mathbf{r} \delta n_+(\mathbf{r} - \mathbf{R}_i) = -\frac{4}{3} \pi r_0^3 \bar{n} N_v = -ZN_v. \quad (14)$$

In contrast to functional (3), functional (11) is three-dimensional, which makes the numerical solution of the optimization problem very laborious.

4. HOMOGENEOUS PSEUDOMETAL

The SJ functional in [13] was constructed using averaging of the electron–ion pseudopotential interaction over the usual Wigner–Seitz cell with a radius r_0 (mean field approximation). Let us do it in a similar way in the case with the presence of vacancies.

We represent the vacancy contribution as the sum

$$\epsilon^{(0)} = T_0 + \langle \delta v_{\text{eff},v} \rangle_v, \quad (15)$$

where T_0 is the energy of the ground state of the electron in a supercell with a radius

$$R_v = r_0 c_v^{-1/3}$$

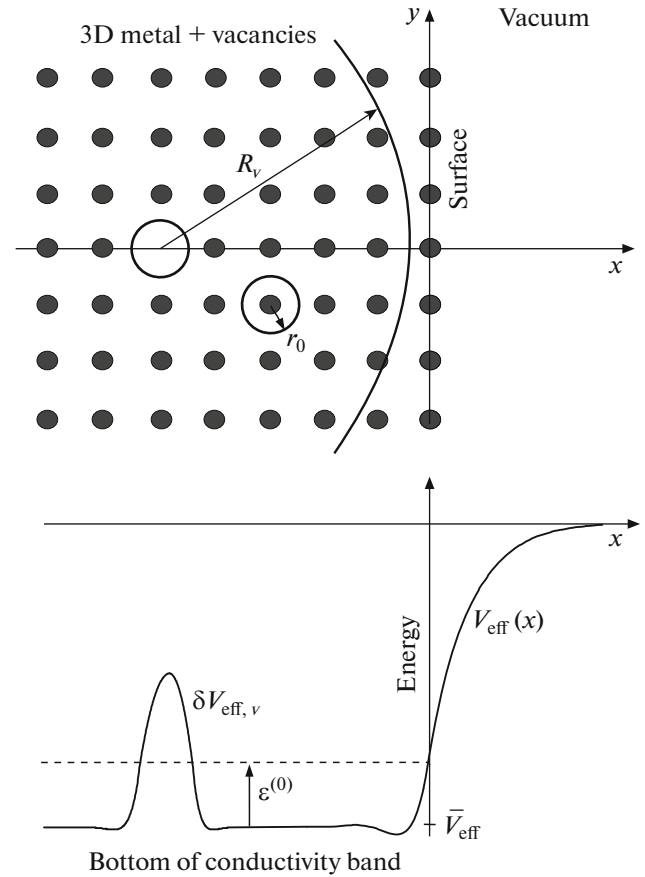


Fig. 1. Profile of an ion lattice with a surface vacancy and energy diagram of electrons.

(the energy is calculated in the zero radius potential approximation) and $\langle \delta v_{\text{eff},v} \rangle_v$ is the supercell bulk averaged contribution of the potential energy from the electron–vacation potential (Fig. 1) [5]. Now, the quantity $\epsilon^{(0)}$ can be included into the functional together with the stabilization potential $\langle \delta v \rangle_{\text{WS}}$.

In accordance with this, we replace (11) by a functional with one-dimensional distribution of charges, as in expression (3):

$$E_{N,v}[n(r)] = \frac{e}{2} \int d\mathbf{r} \phi(r) [n(r) - n_+(r)] + G[n(r)] - \tilde{\epsilon} \int d\mathbf{r} n_+(r) + [\langle \delta v \rangle_{\text{WS}} + \epsilon^{(0)}] \int d\mathbf{r} \theta(r - R_{N,v}) n(r). \quad (16)$$

For functional (16), one can propose an abbreviation SJ + v.

Expressions (3) and (4) distinguish not only by the presence of the zero-point energy $\epsilon^{(0)}$ in (16) but also by the average substance density in the metal for the same N (compare (6) and (12)). The input data of the SJ + v model (16) are r_s , Z , and c_v ($\epsilon^{(0)} \propto c_v$). For such a pseudometal, the pseudopotential core radius r_c must depend on c_v .

For a semi-infinite metal ($R_{N,v}$, $N \rightarrow \infty$; the axis $x = r - R_{N,v}$ is perpendicular to the metal ($x \leq 0$) –vacuum ($x > 0$) interface), the equilibrium profile of electrons $n(x)$ is found as a result of the joint solution of a system of Kohn–Sham equations with the effective potential (Fig. 1)

$$v_{\text{eff}}(x) = e\phi(x) + v_{\text{xc}}(x) + [\langle \delta v \rangle_{\text{WS}} + \varepsilon^{(0)}] \theta(x) \quad (17)$$

and Poisson's equation.

In accordance with (12) and electroneutrality condition for such a pseudometal, the concentration of charges in the metal bulk is lower on the average. As $x \rightarrow -\infty$,

$$n(x) \rightarrow \bar{n} = \bar{n}_+ = \frac{Z\bar{n}_a}{1 + c_v}, \quad (18)$$

where n_a is the density of atoms (ions).

After the calculation of exact profiles of electron and potential distributions, the work function

$$W = -\bar{v}_{\text{eff}} - \bar{\varepsilon}_F, \quad \bar{\varepsilon}_F = \frac{\hbar^2}{2m} (3\pi^2 \bar{n})^{2/3} \quad (19)$$

and specific surface energy

$$\sigma = \sigma_J + [\langle \delta v \rangle_{\text{WS}} + \varepsilon^{(0)}] \int_{-\infty}^0 dx [n(x) - \bar{n}], \quad (20)$$

are calculated. Here, σ_J is the functional corresponding to the usual jellium. It contains the kinetic energy, the exchange–correlation energy, and the electrostatic component. The exact electron profiles corresponding to the minimum of functional (16) should be substituted into this functional.

It is possible to propose an analytical method of solving the problem without direct minimization of functional (16).

5. ANALYTICAL APPROACH

According to the perturbation theory when the presence of vacancies is considered as a small perturbation, under the restriction of the mean field approximation, it is sufficient to use the result of minimization of functional (3) and electron and potential profiles of a defectless metal. Using this procedure is valid when calculating only linear (with respect to c_v) corrections to its characteristics.

Let us represent \bar{n}_+ and \bar{n} in the form

$$\begin{aligned} \bar{n}_+(c_v) &= \bar{n}_+^0 + \bar{n}_+^1 c_v + O(c_v^2), \\ \bar{n}(c_v) &= \bar{n}^0 + \bar{n}^1 c_v + O(c_v^2), \end{aligned} \quad (21)$$

where \bar{n}^0 is the electron density of the defectless metal (coincides with (5)).

From the expansion in small c_v in (18), using (21), we obtain the trivial equalities

$$\begin{aligned} \bar{n}_+^0 &= \bar{n}^0, \\ \bar{n}_+^1 &= \bar{n}^1 = -\bar{n}^0. \end{aligned} \quad (22)$$

In the pseudopotential description of the metal, we also represent

$$r_c(c_v) = r_c^0 + r_c^1 c_v, \quad (23)$$

where r_c^0 corresponds to a defectless metal. The quantity r_c^1 can be easily determined from the equation for the internal pressure in the metal $P = -\bar{n}^2 d\varepsilon/d\bar{n}$. Let us expand P in powers of c_v :

$$P(c_v) = P^0 + \left[\frac{\partial P^0}{\partial \bar{n}^0} \bar{n}^1 + \frac{\partial P^0}{\partial \bar{n}_+^0} \bar{n}_+^1 + \frac{\partial P^0}{\partial r_c^0} r_c^1 \right] c_v + O(c_v^2), \quad (24)$$

where \bar{n}^1 and \bar{n}_+^1 are determined from (22). Using the condition of the absence of metal vapor $P^0 = 0$,

$$P(c_v) = 0, \quad (25)$$

definition of the compression bulk modulus B , and expressions

$$\frac{dP}{d\bar{n}_a} = \frac{\partial P}{\partial \bar{n}} \frac{d\bar{n}}{d\bar{n}_a} + \frac{\partial P}{\partial \bar{n}_+} \frac{d\bar{n}_+}{d\bar{n}_a} = \frac{B}{\bar{n}},$$

we obtain

$$\frac{\partial P^0}{\partial r_c^0} r_c^1 = B^0. \quad (26)$$

At the same time, using (9), we have

$$\frac{\partial P}{\partial r_c} = -4\pi e^2 \bar{n}^2 r_c, \quad (27)$$

which leads to

$$r_c^1 = \frac{-B^0}{4\pi e^2 (\bar{n}^0)^2 r_c^0}. \quad (28)$$

For Al, $r_c^1 \approx -0.05a_0$, where a_0 is the Bohr radius.

The inequality $r_c(c_v) < r_c^0$ can be commented as follows. The appearance of vacancies with the following averaging of the substance density lead to a decrease in the internal pressure in the pseudometal which becomes somewhat rarefied. The pressure becomes negative ($P(c_v) < P_0 = 0$) and the pseudometal loses its stability. According to (27), the pressure can be increased by decreasing the core radius. Therefore, condition (25) is satisfied only at negative values of r_c^1 .

By analogy with resistance (21), we represent the electron work function and surface energy of the metal containing vacancies in the form

$$\begin{aligned} W &= W^0 + W^1 c_v \equiv W^0(1 + \alpha_W c_v), \\ \sigma &= \sigma^0 + \sigma^1 c_v \equiv \sigma^0(1 + \alpha_\sigma c_v), \end{aligned} \quad (29)$$

where $\alpha_W = W^1/W^0$ and $\alpha_\sigma = \sigma^1/\sigma^0$. Then, performing in (19) the expansion in small $\bar{n}^1 c_v$ and using (22), we have for the correction to the work function

$$W^1 c_v = -\frac{dW^0}{d\bar{n}^0} \bar{n}^0 c_v - \varepsilon^{(0)}. \quad (30)$$

Similarly, for surface energy (20), we obtain

$$\sigma^0 = \sigma_J^0 + \langle \delta v \rangle_{\text{WS}}^0 \int_{-\infty}^0 dx [n^0(x) - \bar{n}^0], \quad (31)$$

$$\sigma^1 c_v = -\frac{d\sigma^0}{d\bar{n}^0} \bar{n}^0 c_v + \varepsilon^{(0)} \int_{-\infty}^0 dx [n^0(x) - \bar{n}^0]. \quad (32)$$

Expressions (30)–(32) are the result of successive determination of the vacancy dependence of the work function and surface energy within the framework of the SJ + v model.

6. CALCULATIONS

Table 1 presents the calculated characteristics of a defectless metal and coefficients of first vacancy corrections α_W and α_σ for Na and Al. The derivatives in formulas (30) and (32) were calculated numerically for functional (3) as ratios of the increments ΔW and $\Delta \sigma$ to small negative $\Delta \bar{n}$ at $c_v = 0$. Therefore, the calculations were carried out twice: for r_s^0 (real metal) and for a value r_s (pseudometal) somewhat greater than r_s^0 . Under the assumption $r_c^1 c_v \ll r_c^0$, the dependence $r_c(c_v)$ was not taken into account. In spite of this fact, signs of the derivative in Table 1 reflect both the thermal expansion effect and the effect of elastic mechanical deformation of the metal [17–21], which lead to a decrease in the atom density on the average (W and σ decrease with an increase in r_s (or a decrease in \bar{n}^0)).

The developed approach is simpler and more transparent for analysis than the approach based on sum rules and presented in [7, 8]. It makes it possible to directly work in the Kohn–Sham version and to calculate the corresponding derivatives in (30) and (32) without using the gradient expansion of the functional and manipulations with sum rules [7, 8].

7. EQUILIBRIUM VACANCIES

For a specified temperature T and with the use of the expressions

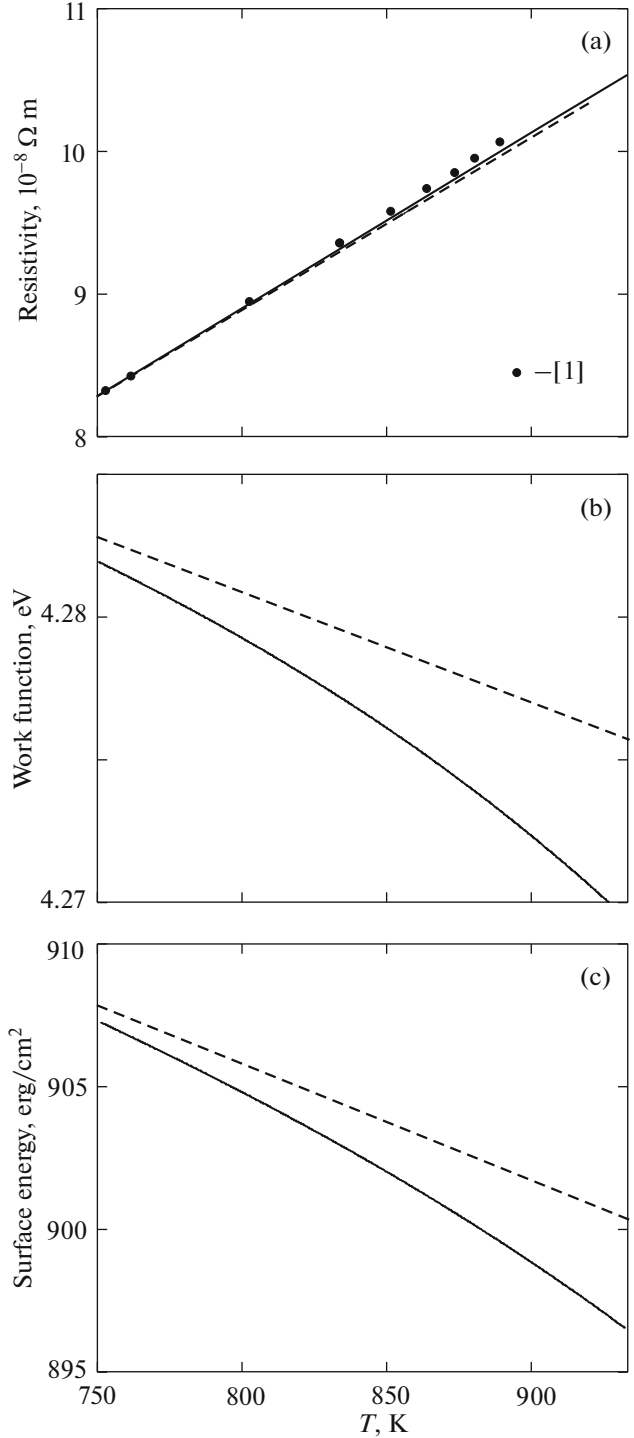


Fig. 2. Temperature dependences calculated for Al by (34)–(36): (a) resistivity ρ (with $\alpha_\rho = 29$ from [5]), (b) electron work function W , and (c) specific surface energy. The dots (the experiment [2]) are in correspondence with the value $\alpha_\rho = 100$ in (34). The dashed lines are the linear temperature dependences (in the formulas, the coefficients $\alpha_\rho, \alpha_W, \alpha_\sigma = 0$).

$$\begin{aligned} c_v(T) &= 1.69 \exp(-\varepsilon_v/k_B T), \\ r_s(T) &= r_s^0 [1 + \lambda(T - T^0) + c_v/3] \end{aligned} \quad (33)$$

for the determination of $\bar{n}^0(T)$ (5), Fig. 2 shows the constructed temperature dependences

$$\rho(T) = \rho^0 [1 + \beta(T - T^0) + \alpha_\rho c_v], \quad (34)$$

$$W(T) = W^0 \left[1 + \frac{dW}{dT}(T - T^0) + \alpha_W c_v \right], \quad (35)$$

$$\sigma(T) = \sigma^0 \left[1 + \frac{d\sigma}{dT}(T - T^0) + \alpha_\sigma c_v \right], \quad (36)$$

where $\lambda = 24 \times 10^{-6} \text{ K}^{-1}$ and $\beta = 4.3 \times 10^{-3} \text{ K}^{-1}$ are the experimental values of the temperature coefficients of linear expansion and electrical resistance, vacancy formation energy $\varepsilon_v = 0.66 \text{ eV}$ [2], and the calculated value of the coefficient $\alpha_p = 29$ from [5] for Al.

The derivatives in formulas (35) and (36) were calculated using (33) as ratios of the increments ΔW_0 and $\Delta \sigma^0$ to small positive ΔT at $c_v = 0$ and $r_c = r_c(T)$. The calculated quantities have a descending temperature dependence. In spite of rather weak changes in the work function in Fig. 2b, it is quite possible to trace its behavior experimentally [22, 23].

The values $\varepsilon^{(0)}$ in (30) and (32), as well as α_p in (34), were calculated within the framework of the same theory [5]. Since the value of α_p turned out to be underestimated by approximately three times as compared to the experiment (dots in Fig. 2a), one can suppose that the calculated values of the coefficients α_W and α_σ in Figs. 2b and 2c are also underestimated. Following this, one can expect that vacancy dependences of the work function and surface energy will manifest themselves in experiments much more considerably than those presented in Fig. 2.

As a result of the proposed approach, the vacancy contribution to the work function and surface energy is expressed only in terms of characteristics of a defectless metal. It is evident that functional (16) in the process of searching vacancy corrections linear in c_v corresponds to the mean field approximation typical for jellium-like models. The idea of a vacancy superlattice presupposes the presence of intervacancy correlations which were not taken into account in this work. Taking them into account requires additional investigations.

REFERENCES

1. N. W. Ashcroft and N. D. Mermin, *Solid State Physics* (Holt, Rinehart and Winston, New York, 1976), Vol. 1.
2. Y. Kraftmakher, *Phys. Rep.* **299**, 79 (1998).
3. C. Freysoldt, B. Grabowski, T. Hickel, J. Neugebauer, G. Kresse, A. Janotti, and C. G. van de Walle, *Rev. Mod. Phys.* **86**, 253 (2014).
4. A. G. Khrapak and S. A. Khrapak, *Low Temp. Phys.* **39**, 465 (2013).
5. A. V. Babich, P. V. Vakula, and V. V. Pogosov, *Phys. Solid State* **56**, 873 (2014).
6. A. V. Babich, P. V. Vakula, and V. V. Pogosov, *Phys. Solid State* **56**, 1726 (2014).
7. V. V. Pogosov, *Phys. Solid State* **59**, 1071 (2017).
8. V. V. Pogosov and V. I. Reva, *J. Chem. Phys.* **148**, 044105 (2018).
9. S. Amelinckx and D. van Dyck, in *Encyclopedia of Materials Science and Engineering*, Ed. by R. W. Cahn (Pergamon, New York, 1988), Vol. 1, p. 77.
10. C. Hock, C. Bartels, S. Straßburg, M. Schmidt, H. Haberland, B. von Issendorff, and A. Aguado, *Phys. Rev. Lett.* **102**, 043401 (2009).
11. M. Itoh, V. Kumar, and Y. Kawazoe, *Phys. Rev. B* **73**, 035425 (2006).
12. R. S. Berry and B. M. Smirnov, *Phys. Rep.* **527**, 205 (2013).
13. J. P. Perdew, H. Q. Tran, and E. D. Smith, *Phys. Rev. B* **42**, 11627 (1990).
14. J. P. Perdew, *Prog. Surf. Sci.* **48**, 245 (1995).
15. J. Bardeen, *Phys. Rev.* **49**, 653 (1936).
16. J. P. Perdew and A. Zunger, *Phys. Rev. B* **23**, 5048 (1981).
17. V. V. Pogosov and V. P. Kurbatsky, *J. Exp. Theor. Phys.* **92**, 304 (2001).
18. C. J. Fall, N. Binggeli, and A. Baldereschi, *Phys. Rev. Lett.* **88**, 156802 (2002).
19. A. V. Babich and V. V. Pogosov, *Surf. Sci.* **603**, 2393 (2009).
20. L. Gao, J. Souto-Casares, J. R. Chelikowsky, and A. A. Demkov, *J. Chem. Phys.* **147**, 214301 (2017).
21. J.-Y. Lee, M. P. J. Punkkinen, S. Schönecker, Z. Nabi, K. Kádas, V. Zólyomi, Y. M. Koo, Q.-M. Hu, R. Ahuja, B. Johansson, J. Kollaár, L. Vitos, and S. K. Kwon, *Surf. Sci.* **674**, 51 (2018).
22. T. Durakiewicz, A. J. Arko, J. J. Joyce, D. P. Moore, and S. Halas, *Surf. Sci.* **478**, 72 (2001).
23. H. Kawano, *Prog. Surf. Sci.* **83**, 1 (2008).

Translated by A. Nikol'skii